Article

Semi-Disparate Impact of Kinases GCN2 and PERK in Modulating the Dynamic Control Properties of eIF2 Pathway

Khan, Mohammad Farhan, Spurgeon, Sarah K., Nofal, Muaffaq and Yan, Xing-Gang

Khan, Mohammad Farhan, Spurgeon, Sarah K., Nofal, Muaffaq and Yan, Xing-Gang (2019) Semi-Disparate Impact of Kinases GCN2 and PERK in Modulating the Dynamic Control Properties of eIF2 Pathway. IEEE Access, 7 . pp. 68132-68139.

http://dx.doi.org/10.1109/ACCESS.2019.2918216

IEEE Access
Multidisciplinary | Rapid Review | Open Access Journal

Received March 11, 2019, accepted May 17, 2019, date of publication May 22, 2019, date of current version June 6, 2019.

Digital Object Identifier 10.1109/ACCESS.2019.2918216

Semi-Disparate Impact of Kinases GCN2 and PERK in Modulating the Dynamic Control Properties of eIF2 Pathway

MOHAMMAD FARHAN KHAN[1,2], SARAH K. SPURGEON[3], (Senior Member, IEEE), MUAFFAQ M. NOFAL[4], AND XING-GANG YAN[5]

[1]School of Engineering, University of Central Lancashire, Preston PR1 2HE, U.K.
[2]International Manufacturing Centre, University of Warwick, Coventry CV4 7AL, U.K.
[3]Department of Electronic and Electrical Engineering, University College London, London WC1E 6BT, U.K.
[4]Department of Mathematics and General Sciences, Prince Sultan University, Riyadh 11586, Saudi Arabia
[5]School of Engineering and Digital Arts, University of Kent, Canterbury CT2 7NT, U.K.

Corresponding author: Mohammad Farhan Khan (farhan7787@gmail.com)

ABSTRACT The tumor microenvironment associated with deficiencies in nutrients and oxygen is important in observing the regulation of tumor progression. The aggressiveness of the tumor cells can be stimulated by exposing it to nutrient starvation and hypoxia. During nutrient starvation, activation of an integrated stress response pathway takes place, which helps tumor cells to cope with nutrient stress. In this paper, an evolutionarily conserved central translational control pathway, i.e., the integrated stress response pathway is analyzed with the help of a mathematical model. This paper is of significant novelty in terms of testable predictions about specific pathway properties with the help of analysis tools from control theory. The investigation has suggested that both kinases GCN2 and PERK have semi-disparate impact on the dynamic control properties of the system. The examples include both kinases show analogous behavior toward the robustness and stability of the system, but disparate behavior in compensating the loss of another kinase.

INDEX TERMS Bode analysis, linear system, mathematical modeling, protein synthesis, robustness, stability, biophysics.

I. INTRODUCTION

Translational and transcriptional regulations are known to control and determine the gene expression levels [1], [2]. The translational activity is solely controlled by numerous translation factors, and broadly occurs in four different stages namely initiation, elongation, termination and recycling. One of the best studied translational control mechanisms impinges on the eukaryotic initiation factor 2 (eIF2) [3].

The eIF2 has a tendency to quantitatively block gene expression levels when phosphorylation of its α-subunit occurs during diverse array of stimuli [4]. Phosphorylation of eIF2α converts eIF2 into competitive inhibitor of eIF2B, which as a result disturbs the guanidine exchange cycle and ceases on-going translation activity [5]. Down-regulation of eIF2 due to excessive phosphorylation is responsible for survival of tumor cell [6], and causes numerous neurological diseases such as Alzheimer [7], Parkinson [8], Huntington [9].

There are various kinases known to phosphorylate eIF2α in response to a diverse array of stimuli such as GCN2, PERK, PKR and HRI [10]. Integrated stress response (ISR) pathway is one of the pathways that constitutes all four kinases and responds during extracellular stimuli [4]. Such array of stimuli trigger changes in the cells by activating kinases, which tend to phosphorylate eIF2α.

Among these kinases, GCN2 is conserved in eukaryotes at both structural and functional levels and activates by interacting with uncharged tRNAs during amino acid deprivation, whereas PERK is activated due to accumulation of unfolded proteins in the endoplasmic reticulum (ER) [11], [12]. Also, it has been found that uncontrolled production of protein under amino-acid deficiency causes accumulation of misfolded peptides in the ER and lead to PERK activation [13]. The similarity between regulation of GCN2 and PERK is that, both kinases have tendency to connect to the output

The associate editor coordinating the review of this manuscript and approving it for publication was Yongjie Li.

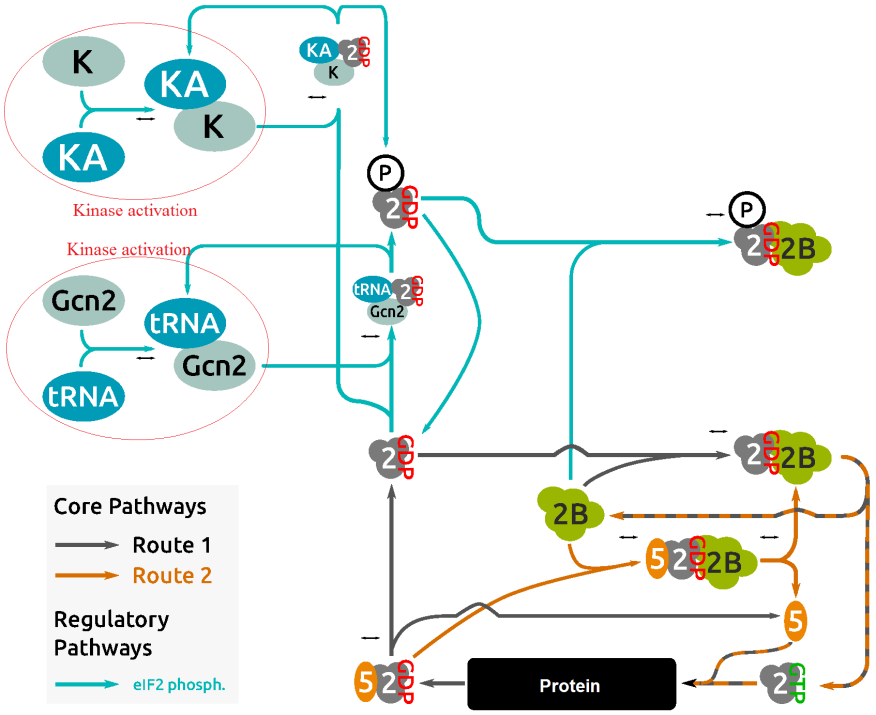

FIGURE 1. eIF2 dependent regulatory pathway representing regulation of translation via phosphorylation of eIF2. Under diverse array of stimuli, the activation of PERK and GCN2 occur, which disrupts the translation activity and sustain cell metabolism. The species indicated in the form of symbols are: 2, eIF2; 2-P, phosphorylated eIF2; 2B, eIF2B; 5, eIF5; K, PERK; KA, misfolded peptide.

of translational activity in a form of feedback loop under amino-acid starvation. On the other hand, the remaining two kinases which are not derived from translational activity are PKR and HRI. PKR activates to double-stranded RNA, while kinase HRI responds to heme deprivation [14]. In this paper, the former group of kinase is mathematically modeled under amino-acid deficiency, and the analysis tools from control theory are used to address the dynamic control properties of the pathway.

The active role of GCN2 and PERK on overall translation activity has been studied extensively in the literature [15]–[19]. To study the role of GCN2 and PERK on translation initiation with the help of mathematical model is possible in two different ways. The first approach is to consider the overall translation initiation pathways, while another approach is to focus on core reactions [20]–[26]. In this paper, a system of core eIF2:GDP complexes is adopted to investigate the semi-disparate role of kinases GCN2 and PERK in modulating the dynamic control properties of the eIF2 system.

The remainder of the paper is organized as follows. In Section II, a mathematical model of eIF2 dependent regulatory system is developed using mass action kinetics. The same section also demonstrate a simple yet effective optimization algorithm for parameter estimation comprising of number of constraints to cope from limited data problem. Section III presents the detailed analyses of the dynamical behavior of eIF2 dependent regulatory system. The analyses presented in this section is novel in terms of testable predictions about specific pathway properties. Finally the paper is concluded in Section IV.

II. MATERIALS AND METHODS

A. MATHEMATICAL MODEL

Fig. 1 illustrates the eIF2 pathway, which comprises of the core reactions required for sustaining ongoing translation activity. The initiation factor eIF2 has an ability to exchange between its GDP-bound and GTP-bound states with the help of guanine nucleotide exchange factor (GEF) termed eIF2B, before it is capable for the next round of translation initiation. The exchange process is further regulated by a guanidine dissociation inhibitor (GDI) function of eIF5 [27]. The release of eIF2:GDP in the form of eIF2:GDP:eIF5 complex indicates completion of translation initiation process [28]. To sustain the ongoing translation activity, regeneration of eIF2:GDP is required by forming eIF2B:eIF2:GDP GEF complex. The formation of eIF2B:eIF2:GDP GEF complex is possible either by release of eIF5 prior to recruitment of eIF2B (route 1) or through eIF5:eIF2B:eIF2:GDP intermediate complex (route 2) [27].

During diverse array of stimuli, phosphorylation of eIF2 converts it into a competitive inhibitor of eIF2B. Phosphorylated eIF2 (eIF2-P) binds with eIF2B to form a tight complex that disrupts nominal translation activity [29]. The proposed model includes two distinct kinases that impact the concentration level of phosphorylated eIF2. The rationale for

considering two kinases is to investigate the theory proposed by Lehman *et al*. [4] after experimental analyses. That is, in the tumor cells, one kinase takes over another kinase when it is inhibited or removed from the system. In the proposed model, active PERK and GCN2 are considered as two kinases that are responsible for phosphorylating eIF2. In the present model, both kinases combine with respective activators and form a Kinase:KinaseActivator complex for further reaction. In the mathematical model, the reaction of kinase activation is controlled by initial concentrations of reacting species.

The overall reaction system of eIF2 cycle is defined in supplementary file S1. To develop a deterministic mathematical model constituting ODEs to describe the aforementioned reaction system, the mass-action kinetic modeling approach is adopted. The overall ODEs of eIF2 mediated regulatory system is given in supplementary file S2.

Note that, the model represents kinase activation by one of the two aforementioned distinct modes which are responsible for phosphorylation of eIF2α, that is, kinases GCN2 and PERK that are generated as part of the translation reaction. The non-linear mathematical model comprising ODEs in supplementary file S2 has been implemented in Matlab and solved using a modified rosenbrock solver (ode23s) [30].

In order to estimate rate constants of the mathematical model, the Levenberg-Marquardt (LM) algorithm [31] is used. Note that, the quantitative experimental data for the model is limited, and hence the rate constants are estimated with the help of the LM algorithm by integrating it with pathway characteristics such as robustness against parametric fluctuations. The parameter estimation process is to be thoroughly discussed in the sub-section II-C.

B. EXPERIMENTAL DATA

The mammalian molecular initial concentration used to estimate the unknown rate constants are given in supplementary file S3. The range of initial molecular concentrations of the species considered in this work lie between $10nM - 1\mu M$ [32]–[34]. The activation of kinases and phosphorylation of eIF2 are simulated by increasing the total cellular concentrations of activators of GCN2 and PERK [35]. The target of 2,000,000 proteins per micro cubic meter is set as the algorithm constraint [32] for parameterization process, which indicate the sustainable translation activity under non-stress case (when kinase is not activated). Note that, the intracellular concentrations were calculated from molecule numbers based on a mammalian protein density or protein mass per volume ≈ 0.2 g/mL, average length in amino acids of a protein ≈ 400 aa/protein and average mass of amino acid ≈ 110 Da/aa [32]–[34].

To estimate the ratio of eIF2α-P to eIF2α in response to a diverse array of stimuli, the adenovirus expressing cre recombinase (Ad-cre) is injected into the right leg muscle of mice, which resulted in the formation of soft tissue sarcomas in nearly 100% of mice [4]. Further to determine if the GCN2 has been activated in the sarcomas, Lehman *et al.* [4] have homogenized tumors and normal muscle from GCN2+/+, GCN2+/−, and GCN2−/− mice and immunoblotted for total and phosphorylated GCN2. Note that, GCN2 +/+ implies an active state of both copies of GCN2, while GCN2 +/− means only one copy (out of two) is active, and the last one GCN2 −/− indicates both copies of GCN2 are inactive.

Observing two different western blot samples of mixed background sarcomas in [4], reveals that reducing the level of GCN2 affects the level of eIF2α-P. The quantified result shows that, for GCN2 −/− the ratio of eIF2α-P to eIF2α yields a significant reduction in the eIF2α-P level. However in C57BL6 tumors, the reduction in GCN2 concentration has no effect on the levels of eIF2α-P.

C. PARAMETER ESTIMATION

In this section, a minimization of temporal error functions (ξ_1 and ξ_2) is adopted for estimating the unknown rate constants of the model, similar to the one reported by Khan *et al*. in [25]. The minimization of error functions are briefly discussed below.

If the value of ξ_1 is close or equal to zero, then this suggests that the experimental data of protein and data value of simulated model are equal and overlapping.

$$\xi_1 = |Y_{1D} - Y_1(\mathbb{V}, \mathbb{C}, t)| \tag{1}$$

where, ξ_1 is an absolute error between experimental and simulated values, Y_{1D} is the experimental data value of translation, $Y_1(\mathbb{V}, \mathbb{C}, t)$ is $in-silico$ experimental value of translation rate obtained after solving ODEs for rate constant obtained using the LM algorithm.

After obtaining a set of rate constants giving $\xi_1 \equiv 0$, the vector of rate constants i.e. $\mathbb{C}$ is perturbed to $\pm 50\%$ from its obtained value, and the error between $Y_1(\mathbb{V}, \mathbb{C}, t)$ and new simulated protein values is recorded. The average value of error ξ_2 can be determined by

$$\xi_2 = \frac{1}{T}\int_0^T \frac{|Y_1(\mathbb{V}, \mathbb{C}, t) - Y_1(\mathbb{V}, \Delta\mathbb{C}, t)|}{\max(Y_1(\mathbb{V}, \mathbb{C}, t), Y_1(\mathbb{V}, \Delta\mathbb{C}, t))}\, dt \tag{2}$$

where, T is the evaluation time and $\Delta\mathbb{C}$ is equal to $\pm 50\%$ of original $\mathbb{C}$ value. The purpose of perturbing the rate constants is to analyze the responsiveness of translation activity. Lower value of ξ_2 defines high robustness against parametric changes [36], [37]. Therefore, the combination of $\mathbb{C}$ giving minimum value of ξ_2 is considered. Note that, this step helps to extract the highly robust parameter sets from other comparatively less robust parameter sets.

The set of rate constants obtained from the parameterization process is given in Supplementary file S4. Fig. 2 shows the deviation of translation activity with respect to its principal behavior. The red bars represent error ξ_2 for non-stress case, while the blue line represents the translation activity for initial concentration values and rate constants reported in supplementary files S3 and S4 respectively. Steady state translation under non-stress conditions in our model captures the robustness of real-life translation against high parametric fluctuations upto $\pm 50\%$ [4].

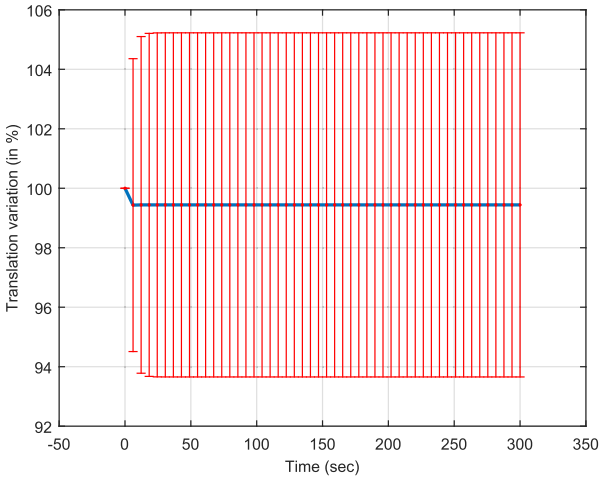

FIGURE 2. Principal behavior and robustness of the non-stress model, when the rate constants of the model undergo fluctuations upto ±50% from its original value. Blue solid line represents principal behavior and red lines represent standard deviation from principal behavior when parameters are fluctuated.

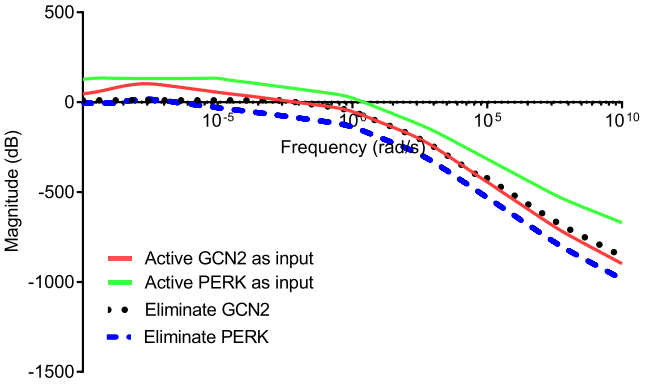

FIGURE 3. Bode magnitude plots by considering activated GCN2 (y_{13}) and PERK (y_{15}) as the inputs. Red solid line represents linear SISO model with active GCN2 as input, while green solid line represents another linear SISO model with PERK as input. The black dotted line and blue dashed line represent behavior of model when GCN2 is removed while PERK is active input and PERK is removed when GCN2 is active input.

III. MODEL ANALYSES AND PREDICTIONS

In this section a semi-disparate behavior of two kinases over dynamic properties of eIF2 dependent regulatory system is analyzed with the help of control theory. The initial concentrations and rate constants obtained for non-stress and stress cases are all the same except the values of Y_{13} and Y_{15}, which are zero (minimum) for non-stress case and greater than zero for stress case respectively. The activation of kinases has a reciprocal effect on changes to the translation activity which resulted into drop of translation activity from ≈2,000,000 proteins/micro cubic meter (100%) to ≈20,000 proteins/micro cubic meter (1%) in a span of 4 minutes.

A. LINEARISATION AND STRUCTURED SINGULAR VALUE ANALYSIS

In this sub-section a non-linear model is linearized around equilibrium point to analyze the frequency behavior of the eIF2 cycle. Note that, the mathematical model is considered as a multi-input single-output (MISO) system, in which formation of protein is system output where the impact of two input kinases is observed. To simulate such model, the transfer functions of MISO model can be considered as two different arrays of elementary single-input single-output (SISO) transfer function: one array resembles uncharged tRNA which actives kinase GCN2 (Y_{13}) as input for one SISO model, while another array resembles active kinase PERK (Y_{15}) as input for another SISO model. Such arrays can help in investigating and comparing the impact of two different kinases individually on general translation activity. Based on ODEs given in supplementary file S2, the generalized state space representation of non-linear SISO model can be defined as follows:

$$\dot{Y}(t) = \hat{\mathbb{Y}}_i\Big(Y(t), \mathbb{C}\Big) + \hat{\mathbb{B}}_i(Y(t))u_i \tag{3}$$

$$Z(t) = Y_1(t) \tag{4}$$

where, $i = [1, 2]$, $\hat{\mathbb{Y}}_1$ is a matrix with $\dot{Y}_{13} = 0$ while $\hat{\mathbb{Y}}_2$ is a matrix with $\dot{Y}_{15} = 0$, vectors $\mathbb{B}_i$ can be represented as:

$$\mathbb{B}_1(Y(t)) = \begin{bmatrix} 0\,0\,0\,0\,0\,0\,0\,0 & -C_{12}Y_9 & C_{12}Y_9 & 0\,0\,0\,0\,0 \end{bmatrix}^T$$

$$\mathbb{B}_2(Y(t)) = \begin{bmatrix} 0\,0\,0\,0\,0\,0 & -C_{20}Y_7 & 0\,0\,0\,0\,0\,0\,0 & C_{20}Y_7 \end{bmatrix}^T,$$

$Z(t)$ is the output (or protein) and vector $\mathbb{C} = \begin{bmatrix} C_1 & C_2 & C_3 & \cdots & C_{22} \end{bmatrix}^T$.

The linearized model of non-linear SISO system around equilibrium point (Y^{eq}) is described below. Note that, the non-linear model is first linearized around equilibrium point Y^{eq} and then the linearized system dynamics are equated to zero. The feasible equilibrium point for the model is given in Supplementary file S5.

The state space representation of approximate linear SISO system around the equilibrium point mentioned in Supplementary file S6 can be re-written in the form:

$$\dot{y} = A_i y + B_i u_i \tag{5}$$

$$Z = Dy \tag{6}$$

where, $i = [1, 2]$, A_i is the Jacobian matrix (given in Supplementary file S7), u_i is input signal, B_i and D are constant input and output matrices respectively defined as follows.

$$B_1 = \begin{bmatrix} 0\,0\,0\,0\,0\,0\,0\,0 & -4.039 & 4.039 & 0\,0\,0\,0\,0 \end{bmatrix}^T \times 10^{-2}$$

$$B_2 = \begin{bmatrix} 0\,0\,0\,0\,0\,0 & -3.955 & 0\,0\,0\,0\,0\,0\,0 & 3.955 \end{bmatrix}^T \times 10^{2}$$

$$D = \begin{bmatrix} 1\,0\,0\,0\,0\,0\,0\,0\,0\,0\,0\,0\,0\,0\,0\,0 \end{bmatrix}$$

Note that, for the sake of simplicity, the linear version of non-linear system Y_i is denoted by y_i. In this case, size of the matrix A_i is 15 × 15. On the other hand, finite values within matrix B_i represent the species on which input is acting and matrix D represents the location at which final impact is to be observed that is protein formation. Fig. 3 compares the frequency behavior of two models for different inputs. Observing Bode magnitude plots of both systems, it can be stated that both active kinase inputs GCN2 and

PERK are impacting the translation activity distinctly during phosphorylation process, which is evident from red and green solid lines in Fig. 3. On the other hand, the frequency analysis shows the partial tracking of red solid line and black dotted line, which indicate that elimination of active GCN2 from the model is compensated by another active kinase PERK, while vice-versa is not justified. In other words, this observation suggests that, the downstream of translation activity due to the activation of kinase GCN2 is different than PERK, and change in the general behavior of the system due to the loss or removal of active kinase GCN2 is not similar to that of loss of activated PERK. Note that, the elimination process has been conducted by using matched DC gain method [25].

The above prediction clearly states the distinct role of both kinases on ceasing translation activity, it is worthy to estimate the impact of individual kinase on the robustness and stability of the system. The robustness and stability analyses will help in further investigating the distinct impact of both kinases on the system properties. The robustness of the system can be analyzed using a tool from control theory known as structured singular value (μ) [38], while stability of the system can be analyzed with the help of pole analysis of linearized system. The μ of the proposed linear eIF2 system is defined as:

$$\mu = \frac{1}{\min\limits_{\Delta}\{\bar{\sigma}(\Delta)|\det(I - M(s)\Delta) = 0 \text{ for } \Delta \in B_{\Delta}\}} \tag{7}$$

where, $\bar{\sigma}$ denotes maximum singular value, M(s) denotes the transfer function of the system and B_{Δ} represents a set of uncertainties Δ. From the above equation it is evident that, the principle at which μ-analysis works is to find the smallest value of $\bar{\sigma}(\Delta)$ which makes $(I - M(s)\Delta)$ singular. When there is no Δ such that $\det(I - M(s)\Delta) = 0$ then $\mu = 0$.

To analyze the robustness of the system, a parametric uncertainty matrix block Δ is introduced into the linear system. Note that, $\Delta = \text{diag}\begin{bmatrix}\delta_{C_1} & \delta_{C_2} & \delta_{C_3} & \cdots & \delta_{C_{22}}\end{bmatrix}$ and $M(s)$ is the transfer function defined as:

$$M(s) = D(sI - A_i)^{-1}B_i \tag{8}$$

Now, introducing Δ into the system changes the rate constant C to $C(1 + \delta_C)$. Recalling the state space representation of perturbed system:

$$\begin{aligned} \dot{\delta y} &= A_i \delta y + B_{0i}\Delta y \\ y &= D_{0i}\delta y \end{aligned} \tag{9}$$

Note that the dimensions of constant matrices B_{0i} and D_{0i} are 15×22 and 22×15 respectively. The matrices B_{0i} and D_{0i} for perturbed linear system with two different inputs are defined in Supplementary file S8.

From Figs. 4 and 5, it is evident that the upper bound of $\mu^{-1} = 1$ for both kinases, which suggest that the robustness of the system is similarly affected by both kinases illustrated in Fig. 1. Observing poles of linearized system in supplementary file S9, a similar observation is also noticed for the stability of the system, that is, the poles of the system with different kinase input are distributed in a very similar fashion,

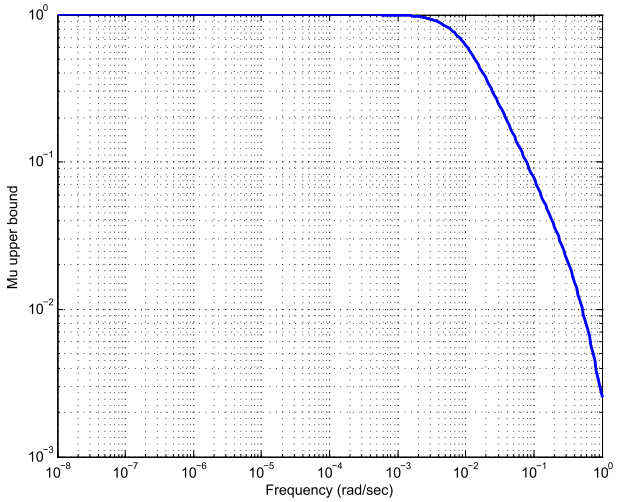

FIGURE 4. Upper bound of the structured singular value μ of linear system (supplementary file S6) with y_{13} as input.

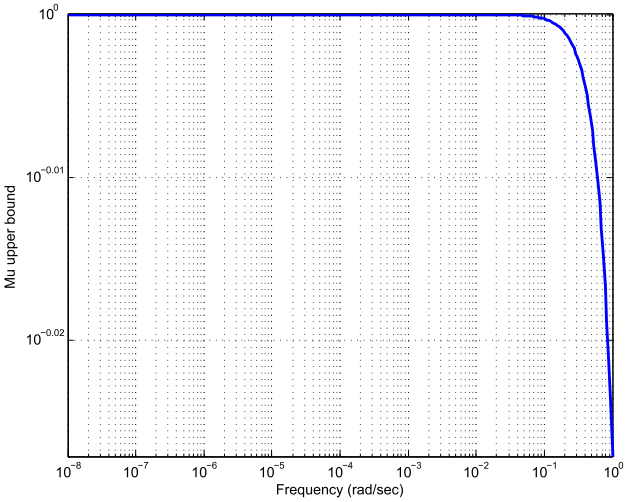

FIGURE 5. Upper bound of the structured singular value μ of linear system (supplementary file S6) with y_{15} as input.

which suggest that the overall stability of the system is also arising from the properties of the common core pathway species. Hence, it can be asserted that, both kinases has analogous impact in terms of robustness and stability of the eIF2 dependent regulatory system.

B. LOSS OF GCN2 ON PHOSPHORYLATION OF eIF2α

It is well understood that under diverse array of stimuli, the activation of kinases GCN2 and PERK take place which leads to formation of Kinase:KinaseActivator complex that phosphorylates eIF2α and form eIF2-P. The mathematical model mimics this particular scenario in a similar way, that is, during the absence of kinase activator complex, the level of eIF2α remains in its steady state and there is no phosphorylation or formation of eIF2-P. On the other hand, during amino acid starvation, the loss in concentration of eIF2α and gain in the strength of eIF2-P take place. It is found that, this process is gradual in nature, that is the ratio of gain/loss in

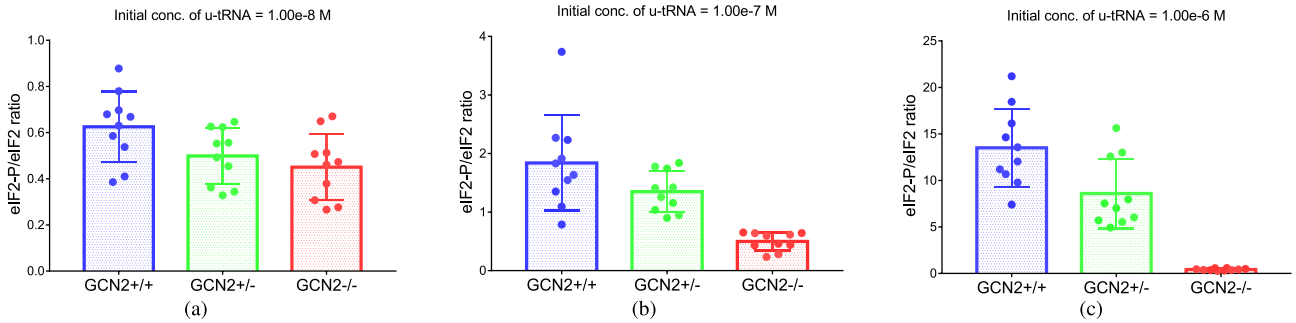

FIGURE 6. Effect of increasing concentration levels of uncharged tRNA on eIF2-P/eIF2α ratio for three different genotypes, while keeping initial concentration of active PERK constant.

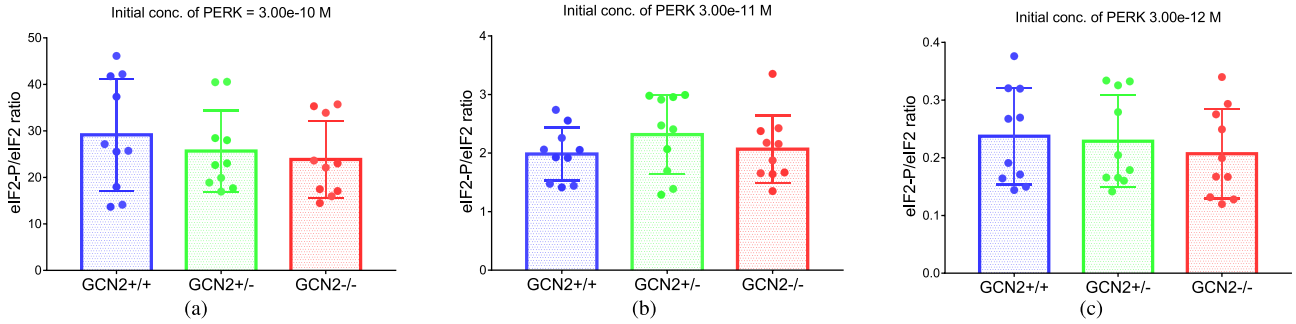

FIGURE 7. Effect of increasing concentration levels of active PERK on eIF2-P/eIF2α ratio for three different genotypes, while keeping initial concentration of uncharged tRNA constant.

eIF2-P/eIF2α largely dependents on the strength of reciprocal effect from starvation.

The Bode plot analysis has revealed that removal of kinase GCN2 has disparate effect on compared to removal of PERK on translation activity. To investigate the effect of loss of GCN2 and tRNA signaling on eIF2-P/eIF2α, the mathematical model performs simulation by considering the concentration of GCN2 as 100%, 50% and 0% of 3.00×10^{-8} M for GCN2 $+/+$, GCN2 $+/-$ and GCN2 $-/-$ respectively. Fig. 6 illustrates the role of strength of uncharged tRNA on eIF2-P/eIF2α ratio. Observing Fig. 6(a) it is found that, lower the pool concentration of uncharged tRNA, lesser will be the statistical significant difference among all three genotypes. On the other hand, higher the pool concentration of uncharged tRNA (Figs. 6(b)-(c)), higher will be the statistical significant confidence limit. This observation reinforces that, variation in tRNA strength is one of the important factor which is responsible for showing statistical significant difference among three genotypes.

In order to further extend this observation, the role of PERK over eIF2-P/eIF2α ratio in Fig. 7 is also illustrated which indicates that, varying concentration of PERK has no impact on statistical significant difference among all three genotypes but drastic increase in strength of eIF2-P. These observations suggest that impact of PERK and GCN2 on the ratio of eIF2-P/eIF2α is distinct, and PERK is compensating the loss of GCN2 and maintaining levels of phosphorylated eIF2α in tumors. Another prediction suggests that one of the reasons behind statistically significant difference between eIF2-P/eIF2α for two different sarcomas is due to the varying strength of uncharged tRNA. This investigation suggests the scenarios in which the removal of kinase has no impact on increase in limit of eIF2α phosphorylation and is therefore not sufficient for derepression of translation activity.

IV. CONCLUSION

In this paper, a mathematical model of eIF2 dependent regulatory model is developed and its dynamic control properties have been addressed. The proposed model consists of two different kinases, which have a tendency to phosphorylate eIF2 in diverse conditions. The mathematical model is able to reach a steady state translational activity at levels very similar to a well-studied $in-vivo$ system, and during activation of eIF2 kinases the translation ceases accordingly. Tools from control theory such as structured singular value and Bode plot analysis have been used to investigate the properties of the system under two kinases namely GCN2 and PERK. The investigations have revealed both kinases has semi-disparate impact on translation activity, that is, both kinases have similar or analogous impact on robustness and stability of the system, whereas disparate impact on the ceasing translation activity. On the other hand, out of the two kinases, only PERK has a tendency to compensate the loss of kinase GCN2 and is responsible for maintaining levels of phosphorylated eIF2α in tumors.

REFERENCES

[1] M. Mathews, N. Sonenberg, and J. Hershey, *Translational Control in Biology and Medicine*. Cold Spring Harbor, NY, USA: Cold Spring Harbor Laboratory Press, 2007.

[2] N. Sonenberg and A. G. Hinnebusch, "Regulation of translation initiation in eukaryotes: Mechanisms and biological targets," *Cell*, vol. 136, pp. 731–745, Feb. 2009.

[3] F. Gebauer and M. W. Hentze, "Molecular mechanisms of translational control," *Nature Rev. Mol. Cell Biol.*, vol. 5, pp. 827–835, Oct. 2004.

[4] S. L. Lehman, S. Ryeom, and C. Koumenis, "Signaling through alternative integrated stress response pathways compensates for GCN2 loss in a mouse model of soft tissue sarcoma," *Sci. Rep.*, vol. 5, Jun. 2015, Art. no. 11781.

[5] A. M. Bogorad, K. Y. Lin, and A. Marintchev, "Novel mechanisms of eIF2B action and regulation by eIF2α phosphorylation," *Nucleic Acids Res.*, vol. 45, pp. 11962–11979, Sep. 2017.

[6] J. Ye, M. Kumanova, L. S. Hart, K. Sloane, H. Zhang, D. N. De Panis, E. Bobrovnikova-Marjon, J. A. Diehl, D. Ron, and C. Koumenis, "The GCN2-ATF4 pathway is critical for tumour cell survival and proliferation in response to nutrient deprivation," *EMBO J.*, vol. 29, pp. 2082–2096, Jun. 2010.

[7] L. Devi and M. Ohno, "Deletion of the eIF2α kinase GCN2 fails to rescue the memory decline associated with Alzheimer's disease," *PLoS ONE*, vol. 8, Oct. 2013, Art. no. e77335.

[8] E. Mutez, A. Nkiliza, K. Belarbi, A. de Broucker, C. Vanbesien-Mailliot, S. Bleuse, A. Duflot, T. Comptdaer, P. Semaille, R. Blervaque, D. Hot, F. Leprêtre, M. Figeac, A. Destée, and M.-C. Chartier-Harlin, "Involvement of the immune system, endocytosis and EIF2 signaling in both genetically determined and sporadic forms of Parkinson's disease," *Neurobiol. Disease*, vol. 63, pp. 165–170, Mar. 2014.

[9] J. Leitman, B. Barak, R. Benyair, M. Shenkman, U. Ashery, F. U. Hartl, and G. Z. Lederkremer, "ER stress-induced eIF2-alpha phosphorylation underlies sensitivity of striatal neurons to pathogenic huntingtin," *PLoS ONE*, vol. 9, Mar. 2014, Art. no. e90803.

[10] N. Donnelly, A. M. Gorman, S. Gupta, and A. Samali, "The eIF2a kinases: Their structures and functions," *Cellular Mol. Life Sci.*, vol. 70, pp. 3493–3511, Oct. 2013.

[11] J. R. Murguía and R. Serrano, "New functions of protein kinase Gcn2 in yeast and mammals," *IUBMB Life*, vol. 64, pp. 971–974, Dec. 2012.

[12] J. Dong, H. Qiu, M. Garcia-Barrio, J. Anderson, and A. G. Hinnebusch, "Uncharged tRNA activates GCN2 by displacing the protein kinase moiety from a bipartite tRNA-binding domain," *Mol. Cell*, vol. 6, pp. 269–279, Aug. 2000.

[13] A. N. Dang, S. R. Kimball, D. R. Cavener, and L. S. Jefferson, "EIF2α kinases GCN2 and PERK modulate transcription and translation of distinct sets of mRNAs in mouse liver," *Physiol. Genomics*, vol. 38, pp. 328–341, Aug. 2009.

[14] J.-J. Chen, "Regulation of protein synthesis by the heme-regulated eIF2α kinase: Relevance to anemias," *Blood*, vol. 109, pp. 2693–2699, Nov. 2006.

[15] E. Sattlegger and A. G. Hinnebusch, "Polyribosome binding by GCN1 is required for full activation of eukaryotic translation initiation factor 2α kinase GCN2 during amino acid starvation," *J. Biol. Chem.*, vol. 280, pp. 16514–16521, Apr. 2005.

[16] M. Dey, B. Trieselmann, E. G. Locke, J. Lu, C. Cao, A. C. Dar, T. Krishnamoorthy, J. Dong, F. Sicheri, and T. E. Dever, "PKR and GCN2 kinases and guanine nucleotide exchange factor eukaryotic translation initiation factor 2B (eIF2B) recognize overlapping surfaces on eIF2α," *Mol. Cellular Biol.*, vol. 25, pp. 3063–3075, Apr. 2005.

[17] Y. Zhang, Y. Wang, K. Kanyuka, M. A. J. Parry, S. J. Powers, and N. G. Halford, "GCN2-dependent phosphorylation of eukaryotic translation initiation factor-2α in Arabidopsis," *J. Exp. Botany*, vol. 59, pp. 3131–3141, Jul. 2008.

[18] J. J. Berlanga, I. Ventoso, H. P. Harding, J. Deng, D. Ron, N. Sonenberg, L. Carrasco, and C. de Haro, "Antiviral effect of the mammalian translation initiation factor 2α kinase GCN2 against RNA viruses," *EMBO J.*, vol. 25, pp. 1730–1740, Apr. 2006.

[19] J. Deng, H. P. Harding, B. Raught, A.-C. Gingras, J. J. Berlanga, D. Scheuner, R. J. Kaufman, D. Ron, and N. Sonenberg, "Activation of GCN2 in UV-irradiated cells inhibits translation," *Current Biol.*, vol. 12, pp. 1279–1286, Aug. 2002.

[20] T. You, G. M. Coghill, and A. J. P. Brown, "A quantitative model for mRNA translation in Saccharomyces cerevisiae," *Yeast*, vol. 27, pp. 785–800, Oct. 2010.

[21] A. S. Spirin, "How does a scanning ribosomal particle move along the 5'-untranslated region of eukaryotic mRNA? Brownian ratchet model," *Biochemistry*, vol. 48, pp. 10688–10692, Oct. 2009.

[22] R. J. Dimelow and S. J. Wilkinson, "Control of translation initiation: A model-based analysis from limited experimental data," *J. Roy. Soc. Interface*, vol. 6, pp. 51–61, Jun. 2008.

[23] T. You, I. Stansfield, M. C. Romano, A. J. Brown, and G. M. Coghill, "Analysing GCN4 translational control in yeast by stochastic chemical kinetics modelling and simulation," *Syst. Biol.*, vol. 5, no. 1, p. 131, 2011.

[24] K. L. Manchester, "Kinetic modelling of the effect of alpha subunit phosphorylation on the activity of the protein synthesis initiation factor eIF-2," *Biochem. Int.*, vol. 22, no. 3, pp. 523–533, Nov. 1990.

[25] M. F. Khan, S. K. Spurgeon, and X.-G. Yan, "Modeling and dynamic behavior of eIF2 dependent regulatory system with disturbances," *IEEE Trans. Nanobiosci.*, vol. 17, no. 4, pp. 518–524, Oct. 2018.

[26] M. F. Khan, S. K. Spurgeon, and T. V. D. Haar, "Origins of robustness in translational control via eukaryotic translation initiation factor (eIF) 2," *J. Theor. Biol.*, vol. 445, pp. 92–102, May 2018.

[27] M. D. Jennings and G. D. Pavitt, "A new function and complexity for protein translation initiation factor eIF2B," *Cell Cycle*, vol. 13, pp. 2660–2665, Sep. 2014.

[28] C. R. Singh, B. Lee, T. Udagawa, S. S. Mohammad-Qureshi, Y. Yamamoto, G. D Pavitt, and K. Asano, "An eIF5/eIF2 complex antagonizes guanine nucleotide exchange by eIF2B during translation initiation," *EMBO J.*, vol. 25, pp. 4537–4546, Oct. 2006.

[29] B. A. Castilho, R. Shanmugam, R. C. Silva, R. Ramesh, B. M. Himme, and E. Sattlegger, "Keeping the eIF2 alpha kinase Gcn2 in check," *Biochim. Biophys. Acta-Mol. Cell Res.*, vol. 1843, pp. 1948–1968, Sep. 2014.

[30] L. F. Shampine and M. W. Reichelt, "The MATLAB ODE suite," *J. Sci. Comput.*, vol. 18, no. 1, pp. 1–22, 1997.

[31] D. W. Marquardt, "An algorithm for least-squares estimation of nonlinear parameters," *J. Soc. Ind. Appl. Math.*, vol. 11, pp. 431–441, Jun. 1963.

[32] R. Milo, "What is the total number of protein molecules per cell volume? A call to rethink some published values," *BioEssays*, vol. 35, pp. 1050–1055, Dec. 2013.

[33] R. J. Ellis, "Macromolecular crowding: An important but neglected aspect of the intracellular environment," *Current Opinion Struct. Biol.*, vol. 11, pp. 114–119, Feb. 2001.

[34] Z. Wang, W. Shen, D. P. Kotler, S. Heshka, L. Wielopolski, J. F. Aloia, M. E. Nelson, R. N. Pierson, Jr., and S. B. Heymsfield, "Total body protein: A new cellular level mass and distribution prediction model," *Amer. J. Clin. Nutrition*, vol. 78, no. 5, pp. 979–984, Nov. 2003.

[35] T. V. D. Haar, "A quantitative estimation of the global translational activity in logarithmically growing yeast cells," *Syst. Biol.*, vol. 2, no. 1, p. 87, Dec. 2008.

[36] K. Asano, T. Krishnamoorthy, L. Phan, G. D. Pavitt, and A. G. Hinnebusch, "Conserved bipartite motifs in yeast eIF5 and eIF2Bϵ, GTPase-activating and GDP-GTP exchange factors in translation initiation, mediate binding to their common substrate eIF2," *EMBO J.*, vol. 18, pp. 1673–1688, Mar. 1999.

[37] J. P. Richardson, S. S. Mohammad, and G. D. Pavitt, "Mutations causing childhood ataxia with central nervous system hypomyelination reduce eukaryotic initiation factor 2B complex formation and activity," *Mol. Cellular Biol.*, vol. 24, no. 6, pp. 2352–2363, Mar. 2004.

[38] J. Kim, D. G. Bates, I. Postlethwaite, L. Ma, and P. A. Iglesias, "Robustness analysis of biochemical network models," *IEE Proc.-Syst. Biol.*, vol. 153, no. 3, pp. 96–104, May 2006.

MOHAMMAD FARHAN KHAN received the B.Tech. and M.Tech. degrees in electronics engineering from the Z. H. College of Engineering and Technology, Aligarh Muslim University, India, in 2010 and 2012, respectively, and the Ph.D. degree in electronic engineering from the School of Engineering and Digital Arts, University of Kent, U.K., in 2017. Since 2017, he has been a Postdoctoral Research Associate in the EPSRC project that is jointly collaborated by the University of Central Lancashire, U.K., and the University of Warwick, U.K. His research interests include control theory application, 3D monitoring, calibration, robotic vision systems, image processing, mathematical modeling, soft computing, machine learning, and computational biology.

SARAH K. SPURGEON (SM'04) received the B.Sc. and D.Phil. degrees from the University of York, York, U.K., in 1985 and 1988, respectively. She is currently a Professor of control engineering and the Head of the Department of Electronic and Electrical Engineering, University College London, U.K. Her research interests include the area of systems modeling, and analysis and robust control and estimation. In these areas, she has published over 270 refereed research papers. She is an OBE. She is a Fellow of the Royal Academy of Engineering, InstMC, IET, and IMA. She is currently a member of the Council of the International Federation of Automatic Control (IFAC) and a member of the General Assembly of the European Control Association. She received the Honeywell International Medal for distinguished contribution as a control and measurement technologist to developing the theory of control, in 2010, and the IEEE Millennium Medal, in 2000. She is the President of the Institute of Measurement and Control.

MUAFFAQ M. NOFAL received the B.S. and M.S. degrees in physics from the University of Jordan, in 1991 and 1995, respectively, and the Ph.D. degree in experimental atomic physics from Frankfurt University, Germany, in 2007. From 2007 to 2009, he was an Assistant Professor with Applied Science University, Amman, Jordan. Since 2009, he has been an Assistant Professor with the Science Department, Prince Sultan University, Saudi Arabia. He has published one book and several articles in his research career. His major research interests include electron spectroscopy, recoil ion momentum spectroscopy, high energy physics, and mathematical modeling of biosystems.

XING-GANG YAN received the B.Sc. degree in applied mathematics from Shaanxi Normal University, in 1985, the M.Sc. degree in control and optimization from Qufu Normal University, in 1991, and the Ph.D. degree in control engineering from Northeastern University, China, in 1997. From 1991 to 1994, he was a Lecturer with Qingdao University, China. He has been a Research Fellow or a Research Associate with Northwestern Polytechnical University, China, The University of Hong Kong, China, Nanyang Technological University, Singapore, and the University of Leicester, U.K. He is currently a Senior Lecturer with the University of Kent, U.K. He has published three books, several book chapters, and over 150 refereed papers. His research interests include sliding mode control, decentralized control, fault detection and isolation, nonlinear control, and time delay systems with applications. He is the Editor-in-Chief of the *International Journal of Engineering Research and Science & Technology* and serves as a member of the Editorial Board for several engineering journals.